



TITLE:

# Fundamental Studies on the Earthquake Resistant Design of Bridge Structures

AUTHOR(S):

GOTO, Hisao

---

CITATION:

GOTO, Hisao. Fundamental Studies on the Earthquake Resistant Design of Bridge Structures. Memoirs of the Faculty of Engineering, Kyoto University 1958, 20(4): 225-236

ISSUE DATE:

1958-12-01

URL:

<http://hdl.handle.net/2433/280418>

RIGHT:

# Fundamental Studies on the Earthquake Resistant Design of Bridge Structures

By

Hisao GOTO

Department of Civil Engineering

(Received August 23, 1958)

## Abstract

This paper describes an outline on the results of fundamental studies on the earthquake resistant design of bridge structures, on which the author has been working since 1948. At first, characteristics of small amplitude vibration of bridge structures are treated theoretically, and at the same time, characteristics of the large amplitude vibration of bridge structures are studied by model tests. Then, from the results obtained above, a fundamental method of computation is derived for the earthquake resistant design. In this case, however, the method of computation may be true only within elastic limits of structural materials and foundation ground. The method of computation for the non-elastic portion is still being studied.

## 1. Introduction

In Japan, comparatively large earthquakes have occurred twelve times since Kanto Earthquake in 1923 which was one of the largest we ever experienced. It is well known that a great number of structures in Japan were damaged by these earthquakes. Damages in bridge structures may be classified as follows; declination and destruction of the abutments, cracking and destruction of the piers, horizontal movement and falling down of the bridge girders, and breakage of the metal fittings of the end bearings. From these observations, it is found that the damages of the bridge structures occur mostly in the substructures of bridges.

Hence, the author puts an emphasis on the studies of earthquake resistant properties or design of structures, considering much of its substructures. Phenomena on the bridge structures accompanied by a strong earthquake motion are so complicated that the author made his plan of studies as follows<sup>1)</sup>; a) Analyze the characteristics of small amplitude vibration by both field tests and the theory within elastic limits of structural materials as well as of the foundation ground. b) Analyze the

characteristics of large amplitude vibration by the model tests. c) Using the results obtained above, find a method of computation for earthquake resistant structures under some reasonable assumptions.

**2. Small Amplitude Vibration of Substructures**

(1) Vibration tests of piers in a field.

Vibration tests were performed on twenty piers and abutments in seven bridges, only the substructures of which had been completed. From the resonance curve by using an oscillator, the following values were obtained:  $T = 0.06 \sim 0.30$  sec,  $\delta = 0.3 \sim 1.2$ , where  $T$  (natural period of piers)  $\cong T_r$  (resonance period of piers), and  $\delta$  is the logarithmic decrement. The dynamic rigidity of the structure including its foundation ground is considered here and is represented in terms of  $y_{cr}/P_{mr}$ , where  $y_{cr}$  is the resonance amplitude at the top of the piers and  $P_{mr}$  the shaking force at resonance point.

(2) Experiments on the foundation coefficient around piers.

The measured values of  $T$  and  $\delta$  obtained above are considerably large, but it is found that these large values are due to the effect of the foundation ground. Hence, the foundation coefficient  $K$  at any depth  $x$  may approximately be expressed by<sup>2)</sup>:

$$K(x) = K_A(x/d)^n$$

where  $K_A$  is the value of  $K(x)$  at  $x=d$ ,  $d$  is the maximum depth of the embedded portion, and  $n$  is the distribution index of  $K(x)$ . From the model test, it is found that  $n=1$  for dry sand and  $n \cong 0.8$  for the ordinary natural ground, and that the large value of the logarithmic decrement  $\delta$  depends mostly on the absorption of the vibration energy caused by the foundation ground.

(3) Theoretical analysis of free vibration of the pier.

Since the piers are known to start vibrating at their embedded portion  $AB$  which is subjected to horizontal earth reactions  $p(x) = K(x)y_1$  in the state of rocking vibration. Hence, for simplicity, we put  $K(x) = K_A(x/d) = K_A(1 - x_1/d)$  from the results in (2), then we get the following fundamental equations of free vibration.

$$\left. \begin{aligned} AB: & E_1 I_1 \frac{\partial^4 y_1}{\partial x_1^4} + b_1 K_A (1 - x_1/d) y_1 + \frac{w_1 a_1}{g} \frac{\partial^2 y_1}{\partial t^2} = 0 \\ BC: & E_2 I_2 \frac{\partial^4 y_2}{\partial x_2^4} + \frac{w_2 a_2}{g} \frac{\partial^2 y_2}{\partial t^2} = 0 \end{aligned} \right\} \dots\dots\dots(1)$$

where  $EI$ ,  $w_a$ , and  $b$  are bending rigidity of structural body, dead weight per unit length, and width, respectively. We can define frequency equation  $F(n) = 0$  and normal function  $u(x)$  by solving these equations simultaneously. And, instead of  $u(x)$ , using a static deflection curve  $\eta$  under a horizontal concentrated load at the top of the pier, we can easily calculate its natural period with good accuracy.

(4) Theoretical analysis of forced vibration of the pier.

Vibration displacement  $y$  of the pier, as shown in Fig. 1, is expressed by the normal function  $u(x)$  and time function  $q$ .

$$\left. \begin{aligned} AB: y_1 &= \sum_{r=1}^{\infty} u_{1r}(x)q_r \\ BC: y_2 &= \sum_{r=1}^{\infty} u_{2r}(x)q_r \end{aligned} \right\} \dots\dots(2)$$

Furthermore, assuming that the earthquake motion is composed of simple harmonic motions  $\sum e_i \sin(p_i t + \phi_i)$ , and applying Lagrange's equation, we get equation (3),

$$\ddot{q}_r + 2\epsilon\dot{q}_r + n_r^2 q_r = \frac{\delta_r}{\Phi_r} \sum k_i \sin(p_i t + \phi_i) \dots\dots\dots(3)$$

where  $\delta_r$  and  $\Phi_r$  are given as the functions of  $u(x)$  obtained from eq. (1), and  $k_i$  is the seismic coefficient. Since eq. (3) can be easily solved, we can compute the vibration displacement  $y$  from eq. (2). In this case, however, a special attention should be paid to the transient stage due to a few simple harmonic motions.

(5) Vibration characteristics of substructures.

It is thus verified both experimentally and theoretically that the vibration characteristics of the bridge are of rocking vibration greatly affected by its foundation ground. The principal effect of the foundation ground on the vibration of bridge piers is due to the elasticity and damping capacity of the ground, both of which are found to have a tendency to increase the values of the natural period as well as of the logarithmic decrement of bridge piers. Furthermore, it is made clear that the fundamental mode of bending vibration is most likely to occur unless the foundation ground is very stiff.

**3. Small Amplitude Vibration of Super- and Sub-structures**

(1) Vibration tests of the bridges in a field.

Vibration tests were performed on ten bridge structures with the oscillator or traffic loads. Common properties of horizontal vibration derived from the results of these tests indicate that effects of the foundation ground on a whole bridge are large as we have seen in case of an individual substructure, and that effects of frictional supporting force at the end bearing part of the bridge girder as well as those of the structural damping in the bridge girder and its end bearing part can not be neglected.

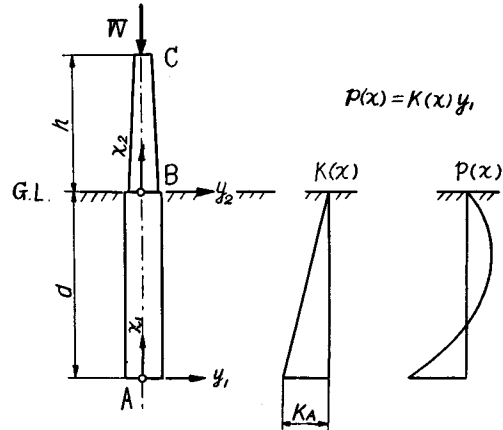


Fig. 1. Illustration of Symbols to the Pier with Well Foundation.

(2) Experiments on the friction mechanism at the end bearing part of bridge.

Values of rolling frictional coefficient  $\mu_r$  and sliding frictional coefficient  $\mu_s$  of the rolling and/or sliding supports of actual bridges are measured in the laboratory. For new bearing supports, we have  $\mu_r = 0.003 \sim 0.006$  and  $\mu_s = 0.14 \sim 0.20$ ; for worn out bearing supports,  $\mu_r = 0.014 \sim 0.025$  and  $\mu_s = 0.16 \sim 0.24$ . However, besides  $\mu_r$  and  $\mu_s$ , there are a few more factors which would be considered to govern characteristics of the friction mechanism.

(3) Theoretical analysis of coupled vibration of the few span bridge.

For a one span bridge subjected to the seismic motion  $e \cos pt$  parallel to the bridge axis as shown in Fig. 2 (a), a vibrating model was set up as in Fig. 2 (b). Here the spring, vibrating mass, damping and seismic forces etc. of the substructures ABC are all converted into the condition at the top of the structures. Thus, we get the following equations,

$$\left. \begin{aligned} M_l \ddot{y}_{cl} + c_l \dot{y}_{cl} + k_l y_{cl} \pm F &= k_0 W_l' \cos (pt - \alpha) \\ M_r \ddot{y}_{cr} + c_r \dot{y}_{cr} + k_r y_{cr} \pm F &= k_0 W_r' \cos (pt + \phi_r - \alpha) . \end{aligned} \right\} \dots\dots\dots (4)$$

A steady state solution of eq. (4) is obtained by approximation. On the other hand, for the seismic motion acting perpendicular to the bridge axis, we regard the bridge girder as a plate spring  $k$  with large rigidity, another vibrating model is set up as in Fig. 3 (b), and the equations in this case are as follows ;

$$\left. \begin{aligned} M_l \ddot{y}_{cl} + c_l \dot{y}_{cl} + k_g (y_{cl} - y_{cr}) &= k_0 W_l' \cos pt \\ M_r \ddot{y}_{cr} + c_r \dot{y}_{cr} + k_r y_{cr} + k_g (y_{cr} - y_{cl}) &= k_0 W_r' \cos (pt + \phi_r) . \end{aligned} \right\} \dots\dots\dots (5)$$

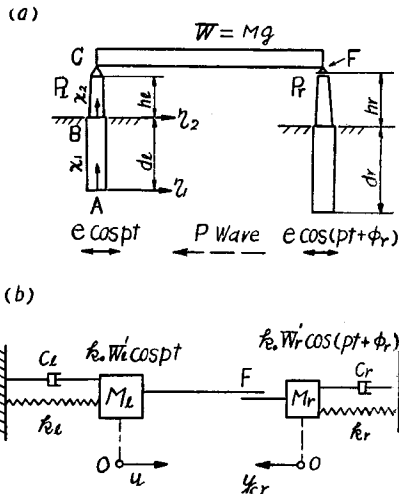


Fig. 2. One Span Bridge and its Vibrating Model. (Parallel to Bridge Axis)

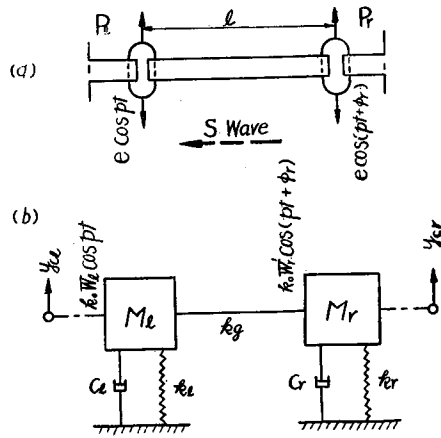


Fig. 3. One Span Bridge and its Vibrating Model. (Perpendicular to Bridge Axis)

For Fig. 3 (b), it is possible to compute the transient vibration, and this method is applicable to the case of two span bridges. The numerical computation of the above equations leads us to the results that effects of the coupled restriction by frictional supporting force  $F$  are not so large, and that effects of the phase angle of seismic motion  $\phi$  on the coupled stationary amplitude are not so large either. But it is very difficult to get clear solutions on the characteristics of the body force of bridge girder itself, the structural damping of the end bearing part of bridge girder, and the transient vibration of eq. (4).

(4) Approximate analysis of multi-span bridges.

The method in (3) is hardly applicable to the case of multi-span bridges. Therefore, under the assumption that the super- and sub-structures are connected with hinges and limited to one degree of freedom, an approximate solution is obtained by Rayleigh's method. It is found that this method gives comparatively reasonable computed values if type and dimensions of the bridge structures are suitable.

(5) Vibration characteristics of super- and sub-structures.

From the above analysis it is made clear that vibration characteristics of super- and sub-structures of bridges are affected largely by the foundation ground and bearing parts of the bridge girder. But it is hard to express mathematically the restoring force and the body force of the bridge girder itself, and the structural damping in the bridge girder and its bearing part. For this reason, next convenient methods are used for actual computation, that is, a) to take individual substructures loaded at their tops with the dead weight of one span girder, b) to restrict the whole bridge into a one degree of freedom system assuming that every bearing part of the bridge girder is of hinged or clamped combination, c) then to estimate actual states lying somewhere in between the results in a) and b)<sup>2)</sup>.

The author has an opinion that it would not give so large errors if the results from a) are taken when the seismic force acts parallel to the axis of bridge with rolling supports, and the results from c) when it acts parallel to the axis of bridge with sliding supports, and the results from b) when it acts perpendicular to the axis of bridge with both supports.

#### **4. Model Tests on a Large Amplitude Vibration**

(1) Outline of model tests.

Since the characteristics of the large amplitude vibration are, of course, important to the earthquake resistant problems, the model tests were performed in the laboratory. In the tests, model piers and model bridges were constructed so that they satisfied the similarity law as closely as possible, and were subjected to the vibrating forces on a shaking table. Vibration records were taken with a dynamic strain recorder by

using wire strain gauges, and readings of strain were converted into the displacement of vibration, that is, for the model piers the deflection meter using strain gauges as given in Fig. 4, and for the model bridge the strain gauges were attached to the plate spring itself of the vibrating model as shown in Fig. 5 (b).

(2) Tests on individual substructure.

Vibration tests were performed on a hollow steel pier in a sand bed set on the shaking table. For the sand bed, coarse and fine sands were used at both states, dry and saturated with water, and as filling materials of the hollow steel pier, four kinds of materials were used, that is, air, water, dry sand, and water-saturated sand. For each combination, a strong excitation was applied to the model until the acceleration exceeded the amount of the gravitational acceleration  $1g=980\text{ cm/sec}^2$ . The results

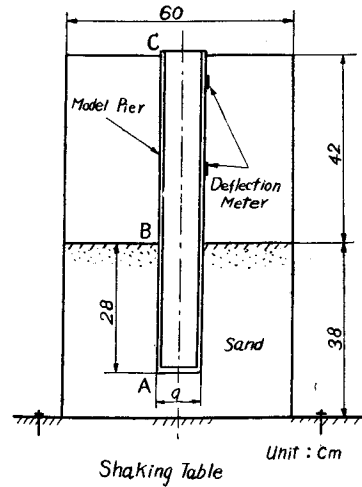
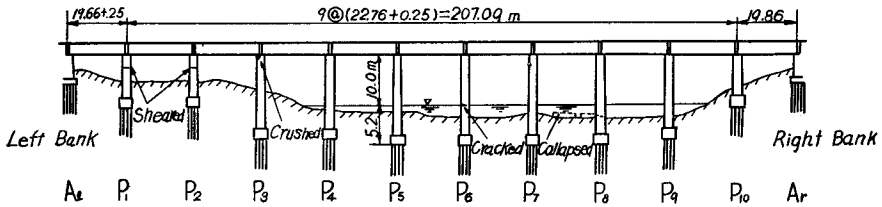
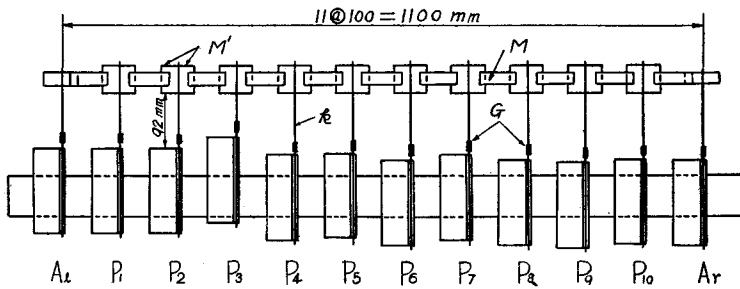


Fig. 4. General View of the Model Test Set-up of a Pier.

(a) Prototype: Nakatsuno Bridge (Scale: - Vertical: Horizontal = 2:1)



(b) Vibrating Model (Parallel to Bridge Axis)



$M$ : Mass of Girder,  $M'$ : Mass of Pier,  $G$ : Strain Gauge,  $k$ : Plate Spring

Fig. 5. Multiple Span Bridge with Sliding Supports and its Vibrating Model.

obtained by this test were that the vibrating characteristics of the piers verified to be of rocking vibration and the logarithmic decrement  $\delta$  ranged in between 0.37 and 1.24 as in 2., (1), and that at 1*g* the resonance period  $T_r$  increased as much as 50 to 60% of that under the weak deflective vibration. As the general tendency, it is observed that the vibration characteristics are linear phenomena when the seismic coefficient is smaller than 0.1, and non-linear when the seismic coefficient is larger than 0.3. And, further observations lead us to the conclusion that more advantage we can get against the vibration if coarser sand is used as a filling material in the well structure of actual piers on a sandy ground.

(3) Experiments on the bridge with sliding supports.

A vibration model was constructed as in Fig. 5 (b), so that tests for the seismic force acting parallel to the axis of the prototype, Nakatsuno Bridge, as shown in Fig. 5 (a). The pier including its embedded portion is taken as spring  $k$ , vibrating mass  $M'$ , and dash-pot  $c$ , and then they are connected with vibrating mass  $M$  of the bridge girder. During the tests, values of  $k$  and  $c$  are adjusted so that natural period  $T$ , mass ratio  $M/M'$  and logarithmic decrement  $\delta$  of each pier meet closely with the estimated values obtained from the results of the prototype experiments. Thus, after the vibration tests within a small amplitude, the strong deflective vibration was applied to the model, which verified the earthquake damages of  $P_1, P_2, P_3$  in Fig. 5 (a) by approximation. The similar tests were done on the model on which the seismic force acted perpendicularly to the axis of the bridge. These explained fairly clear the earthquake damages of  $P_6$  and  $P_8$  in Fig. 5 (a).

(4) Experiments on the bridge with rolling supports.

In this case, the spring  $k$  for the pier, vibrating mass  $M'$ , dash-pot  $c$ , vibrating mass of the bridge girder  $M$ , were used like in (3), but the rolling supports were added with small pullies between  $M'$  and  $M$ . The tests were performed for three cases of five spans, three spans, and single span. The results obtained in these tests show that each pier vibrates nearly individually when the supports roll under the action of large seismic forces which can be the object of the earthquake resistant computation. However, the effects of the body force of the bridge girder  $M$  are pretty large, then each girder can not be taken only as a vibrating particle.

(5) Characteristics of the large amplitude vibration.

A summary of the results of the model tests subjected to the strong deflective vibration is stated below. As the individual substructure, the model has rocking vibration affected by its foundation ground. The bridge with rolling supports has the complicated vibration characteristics depending upon the frictional supporting force at the supports and on the magnitude of the driving force. But, when the seismic force acts in the direction perpendicular to the axis of the bridges, it is noticed that



the vibration of the bridge as a whole is considerably distinguished. Thus, for the studies on the method of earthquake resistant computation, it is obvious that these test results are to be taken into consideration.

**5. Consideration on the Earthquake Resistant Computation**

(1) Assumptions made in the author's method of computation.

It is more difficult to establish the method of earthquake resistant computation directly, considering every characteristics mentioned above. So the author has studied on the practical methods under the following assumptions. 1) The relation between a restoring force and a displacement of substructures is approximately linear<sup>4)</sup>. 2) Beam theory is applied here from the results of the experiments by photo-elasticity. 3) Seismic coefficient theory is taken from the practical point of view. 4) Design seismic motion is considered to be a few cosinusoidal waves. 5) As to the earth reaction acting on the substructures, the results in the model tests are taken as important factors. 6) In calculation of the embedded length, bending moment and shearing force of substructures, and their elastic deformations are neglected.

(2) Static computation of the substructure.

As the earth reactions against the horizontal seismic force ( $k_0$ : seismic coefficient), three factors  $p$ ,  $q$  and  $f$  are chosen as in Fig. 6, where  $p$  is the horizontal earth reaction,

$q$  the earth reaction on the bottom of well structure, and  $f$  the frictional force on the side surface of well structure<sup>5)</sup>. At first, the embedded length  $d$  is required so that the local maximum value  $p_1$  of  $p$  does not exceed the passive earth pressure and the greatest value  $q_1$  of  $q$  does not exceed the allowable bearing force there. The determining equation in this case is an algebraic equation of a high degree of  $d$ . Actually, the equation is the fifth degree of  $d$  since the seismic force acts in the direction of major diameter  $b$  if we neglect the value of  $f$  as shown in Fig. 6. On the other hand, for the computation of bending moment and shearing

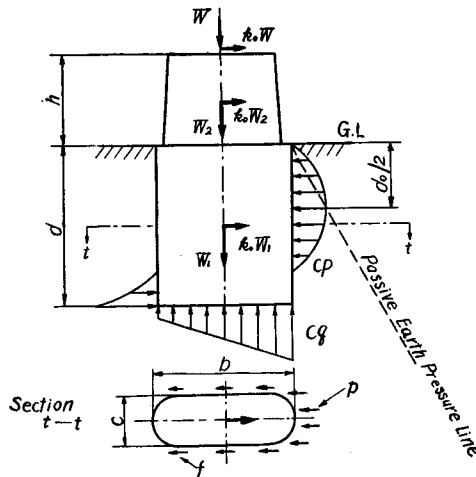


Fig. 6. Diagram of the Earth Reaction Forces Acting on the Well Foundation.

force of the structural body, only  $p$  is considered since the direction of the minor diameter  $c$  of the geometrical moment of inertia is important, and  $q$  and  $f$  affect little as the earth reactions. Thence, the bending moment and shearing force are given by Dr. Mononobe's equation well known in Japan.

(3) Practical computed values on vibration effects.

The fundamental equations of vibrating piers under the seismic motion are given in eq. (3) using a time function. For simplicity, the vibration is converted into one degree of freedom at the top point C of piers, and is taken as the cosinusoidal wave. Thus we get,

$$\ddot{q}(t) + 2\epsilon\dot{q}(t) + n^2q(t) = k_0n^2 \cos (pt + \phi) \dots\dots\dots(6)$$

where response  $q(t)$  can be computed by an analog computer when repetition number  $N$  of  $\cos pt$  is taken for  $N=1/2, 1, 2, 3, \dots$  etc. From the equation, we get the largest value  $q_m(t)$  and compute the ratio of  $q_m(t)$  to  $q_s$  (statically computed value of  $q$ ),  $q_m(t)/q_s=1+D$ . Furthermore, the value of  $(1+D_d)$  is also checked when the factor of danger  $F(q)$  is allowed for in  $q_m(t)$ . Since the ratio of seismic period  $T_p$  to natural period  $T_n$  of substructure should be somewhere in between 2 and 5 for design shall be made within the range of  $1+D_d \cong 1.10 \sim 1.30$  for  $N=1$  or 2,  $F(q)=10\%$ , and logarithmic decrement  $\delta=0.3$  to 1.2.

(4) Dynamic computation of the substructure.

Vibration displacement  $y$  of the pier is expressed in the eq. (2), and if the vibration is restricted to one degree of freedom neglecting the elastic deformation, we get,

$$y = u(x)q(t) = \eta(x)q(t) \dots(7)$$

where  $\eta(x)$  is determined by the earth reactions and seismic force  $k(x)w_a$  due to the seismic coefficient of the structure  $k(x)$  as given in Fig. 7, that is, the displacement  $\eta_c$  at the top C is proportional to  $k'$ , and  $\eta_c$  is the ratio of seismic force  $k_0W_c'$ , converted into the top part,

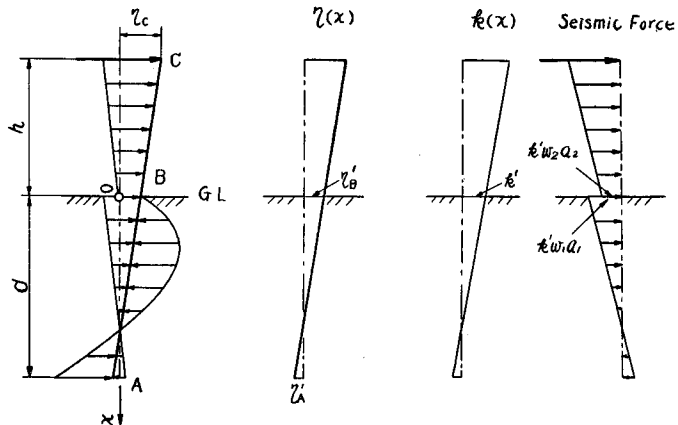


Fig. 7. Illustration of the Actual Seismic Force Acting on the Bridge Substructures.

to spring coefficient  $k_c$ . Thus we obtain,

$$k'\eta_c' = \eta_c = k_0W_c'/k_c \quad \therefore k' = k_0W_c'/k_c\eta_c' \dots\dots\dots(8)$$

from which the seismic coefficient of the structure  $k'$  at the ground surface can be calculated for the seismic coefficient in the foundation. This gives us the seismic force and then  $\eta(x)$ . The bending moment  $M_x$  and shearing force  $S_x$  are obtained from the following equations.

$$\left. \begin{aligned} S_x &= S_B + \frac{1}{2} k' w_1 a_1 \left( 2 + \frac{\eta_{A'}}{\eta_{B'}} \frac{x}{d} \right) x - b \int_0^x p(\xi) d\xi, \\ M_x &= \int S_x dx + c = M_B + \int_0^x S \xi d\xi. \end{aligned} \right\} \dots\dots\dots(9)$$

Under the linearized assumptions, eq. (7) can be applied directly to  $M$  and  $S$ . So, computed dynamical values of  $M_{xd}$  and  $S_{xd}$  are found from eq. (8) multiplied by  $(1+D)$  or  $(1+D_d)$  in (3).

$$\left. \begin{aligned} M_{xd} &= (1+D_d)M_x \cong (1.10 \sim 1.30)M_x \\ S_{xd} &= (1+D_d)S_x \cong (1.10 \sim 1.30)S_x \end{aligned} \right\} \dots\dots\dots(10)$$

(5) Checking the bridge as a whole.

It is thought that there would not be a big error in taking the method shown in (2), (3) and (4) for the bridge with rolling supports. For the bridge with sliding supports, the whole bridge is transformed into a mass and spring system modeled as stated in 3, and displacement  $\eta_c$  at the top  $C$  of each substructure is calculated with the horizontal seismic force acting on the body. The smaller the displacement  $\eta_c$  of structure, the more easily we can get a large seismic force from the whole bridge. In either case, this takes the form of the product of the value in (4) and correcting coefficient  $\alpha \propto 1/\eta_c$ . Hence, the computed value in (4) should be corrected only for the substructure whose  $\alpha$  is greater than unity,  $\alpha > 1.0$ .

(6) Application of the author's method

The third pier of Kuzuryu Bridge is taken as an example. For  $k_0=0.2$ ,  $d=14.2\text{m}$  when only  $p$  is considered, and  $d=6.5\text{m}$  when both  $p$  and  $q$  are taken in account. In practice, however, since the pier is constructed for  $d=13.0\text{m}$ , it can be said to be stable for  $k_0=0.3 \sim 0.4$ . Hence, if taking  $k_0=0.3$ , we get  $k'=0.216$  from eq. (8).

Thus, taking the ordinary computed values of  $M$  and  $S$  in Dr. Mononobe's equations as 100, the values from eq. (9) and eq. (10) are compared and tabulated below. For  $(1+D_d)=1.20$ , the values of  $M_m$  and  $S_m$  in the author's equation are larger than those of ordinary method by 30~40%. It is noticeable that the ordinary method gives the non-safe values for  $M_m$  and  $S_m$ .

Table 1. Computed Values of  $M_m$  and  $S_m$  by Two Methods

|                 | Equations      | $M_m$ | $S_m$ | Remarks      |
|-----------------|----------------|-------|-------|--------------|
| Ordinary Method | Mononobe's Eq. | 100   | 100   | $k_0=0.30$   |
| Author's Method | Eq. (9)        | 116.0 | 106.3 | $k'=0.216$   |
|                 | Eq. (10)       | 139.3 | 128.3 | $1+D_d=1.20$ |

6. Conclusions

The author has discussed the outline of the fundamental results of his study on the earthquake resistant design of the bridge structures. However, there still remain many problems to be studied. For the purpose of completing this task, the author continues his study on the non-elastic vibration due to the strong seismic motion, and on the computation method of the earthquake resistant design by the limit design theory stressing on ultimate strength of materials.

Acknowledgments

The author is very grateful to Professor Ichiro Konishi and Professors in the Department of Civil Engineering, Kyoto University, for their useful advices during the process of this investigation.

References

- 1) H. Goto: Fundamental Studies on Earthquake-proof Design of Bridge Structures, Journal of the Japan Society of Civil Engineers, Vol. 43, No. 7, pp. 25-31, July 1958.
- 2) L. A. Palmer and J. B. Thompson: The Earth Pressure and Deflection of Piles along the Embedded Lengths of Piles Subjected to Lateral Thrust, Vol. 5, pp. 156-161, June 1948.
- 3) I. Konishi and H. Goto: A Dynamical Consideration on Earthquake Damages of Bridge Piers, The Memoirs of the Faculty of Eng., Kyoto University, Vol. 13, No. 2, pp. 77-93, March 1951.
- 4) V. Karmalsky and G. Korner: Design of Bridge Piers Embedded in Cohesionless Material, Taking into Account their Flexibility, Proc. of the Institution of Civil Engineers, No. 2, Vol. 5, Part 3, pp. 535-554, Aug. 1956.
- 5) A. Hirai: Earthquake Resistant Design of Bridge Substructures, Proc. of the World Conference on Earthquake Engineering, pp. 30.1-30.13, June 1956.

Appendix

— A Study on the Limit Design of Bridge Substructures —

It is hoped that the limit design of bridge substructures be studied of the bending moment, shearing force and resistant moment. For the computation of bending moment and shearing force at the critical state, further examination may be needed on the distribution of the earth reaction in Figs. 6 and 7. On the other hand, for the computation of the resistant moment the critical state as shown in Fig. 8 is established,

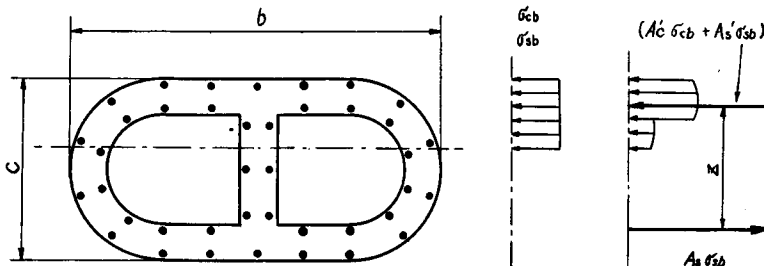


Fig. 8. Stress Diagram of Assumed Condition of the Ultimate Stress in a Well Section.

and the following three conditions are derived using the symbols:  $A_s, A_s'$ ; total cross-sectional area of tensile and compressive reinforcement,  $A_c'$ ; concrete area of compressive strength,  $A, A_0$ ; total area of reinforcement and concrete respectively,  $\sigma_{sb}, \sigma_{cb}$ : ultimate compressive strength of steel and concrete.

$$\left. \begin{aligned} A_s + A_s' &= A, & A_s'/A &= A_c'/A_0 \\ A_s' \sigma_{sb} + A_c' \sigma_{cb} &= A_s \sigma_{sb}. \end{aligned} \right\} \dots\dots\dots(11)$$

Since  $A, A_0, \sigma_{cb}, \sigma_{sb}$  are all given, the unknown quantities  $A_s, A_s', A_c'$  can be obtained from eq. (11). When the position of the neutral axis is found, the acting point of each resultant force is determined, and then the distance between both resultant forces is finally obtained. Thence, the ultimate resistant moment  $M_b$  is expressed in eq. (12);

$$M_b = A_s \sigma_{bs} Z, \quad M = M_b/s \quad \dots\dots\dots(12)$$

where  $s$  is the safety factor.

Therefore, the design is to be done in such way that the bending moment due to the design seismic force coincides the value of  $M$  in eq. (12).